
Distributed Learning of Neural Networks using Independent Subnet Training

Binhang Yuan
 Rice University
 Houston, TX 77005
 by8@rice.edu

Chen Dun
 Rice University
 Houston, TX 77005
 cd46@rice.edu

Anastasios Kyrillidis
 Rice University
 Houston, TX 77005
 anastasios@rice.edu

Christopher M. Jermaine
 Rice University
 Houston, TX 77005
 cmj4@rice.edu

Abstract

Distributed machine learning (ML) can bring more computational resources to bear than single-machine learning, reducing training time. Further, distribution allows models to be partitioned over many machines, allowing very large models to be trained—models that may be much larger than the available memory of any individual machine. However, in practice, distributed ML remains challenging, primarily due to high communication costs. We propose a new approach to distributed neural network learning, called independent subnet training (IST). In IST, a neural network is decomposed into a set of subnetworks of the same depth as the original network, each of which is trained locally, before the various subnets are exchanged and the process is repeated. IST training has many advantages over standard data parallel approaches. Because the subsets are independent, communication frequency is reduced. Because the original network is decomposed into independent parts, communication volume is reduced. Further, the decomposition makes IST naturally “model parallel”, and so IST scales to very large models that cannot fit on any single machine. We show experimentally that IST results in training time that are much lower than data parallel approaches to distributed learning, and that it scales to large models that cannot be learned using standard approaches.

1 Introduction

Distributed neural network (NN) training over a compute cluster has become an essential task in modern computing systems [1, 2, 3, 4, 5]. Distributed training algorithms may be roughly categorized into *model parallel* and *data parallel*. In the former [2, 5], different compute nodes are responsible for different parts of a NN. In the latter [6, 7, 8], each compute node updates a complete copy of the NN’s parameters on different data. In both cases, the obvious way to speed up learning is to add more nodes. With more hardware, the model is split across more CPUs/GPUs in the model parallel setting, or gradients are computed using fewer data objects per compute node in the data parallel setting.

Due to its ease-of-implementation, data parallel training is most commonly used, and it is better supported by common deep learning software, such as TensorFlow [9] and PyTorch [10]. However, there are limitations preventing data parallelism from easily scaling out. Adding nodes means that each node can perform forward and backward propagation more quickly on its own local data, but it leaves the synchronization step no faster. In fact, if synchronization time dominates, adding more machines could actually make training even *slower* as the number of bytes transferred to broadcast an

updated model grows linearly with cluster size. This is particularly problematic in public clouds, such as Amazon EC2¹, that tend to couple relatively slow interconnects with high-performance GPUs, meaning that transfer costs dominate. One can increase batch size to decrease the relative cost of the synchronization step, but this can introduce statistical inefficiency. While there is some debate about the utility of large-batch methods in practice [11, 12], very large batch sizes often do not speed up convergence, and large batches can also hurt generalizability [13, 14, 15, 16, 17, 18, 19].

Independent subnet training. The central idea in this paper, called *independent subnet training* (IST), facilitates combined model and data parallel distributed training. IST utilizes ideas from dropout [20] and approximate matrix multiplication [21]. IST decomposes the NN layers into a set of *subnets* for the same task, by partitioning the neurons across different sites. Each of those subnets is trained for one or more local stochastic gradient descent (SGD) iterations, before synchronization.

Since subnets share no parameters in the distributed setting, synchronization requires no aggregation on these parameters, in contrast to the data parallel method—it is just an exchange of parameters. Moreover, because subnets are sampled without replacement, the interdependence among them is minimized, which allows their local SGD updates for a larger number of iterations, before synchronizing. This reduces communication frequency. Communication costs per synchronization step are also reduced because in an n -machine cluster, each machine gets between $\frac{1}{n^2}$ and $\frac{1}{n}$ of the weights—contrast this to data parallel training, when each machine must receive *all* of the weights.

IST has advantages over model parallel approaches. Since subnets are trained independently during local updates, no synchronization between subnetworks is required. Yet, IST inherits the advantages of model parallel methods. Since each machine gets just a small fraction of the overall model, IST allows the training of very large models that cannot fit into the RAM of a node or a device. This can be an advantage when training large models using GPUs, which tend to have limited memory.

Experimental findings. We evaluate IST on speech recognition, image classifications (CIFAR100 and full ImageNet), and a large-scale Amazon product recommendation task. We find that IST results in up to a $10\times$ speedup for time-to-convergence, compared to a state-of-the-art data parallel realization, using bandwidth-optimal ring all-reduce [22], as well as the “vanilla” local SGD method [23]. Because IST allows for efficient implicit model parallel training, we show that IST can solve an “extreme” Amazon product recommendation task with improved generalization, by increasing the embedding dimensions for larger models, which is not supported by data parallel based training.

2 Preliminaries

NN training. We are interested in optimizing a loss function $\ell(\cdot, \cdot)$ over a set of labeled examples; the loss $\ell(w, \cdot)$ encodes the NN architecture, with parameters w . Given samples $X := \{x_i, y_i\}_{i=1}^n$, deep learning aims in finding w^* that minimizes the *empirical loss*:

$$w^* \in \arg \min_w \frac{1}{n} \sum_{i=1}^n \ell(w, \{x_i, y_i\}). \quad (1)$$

Formula (1) is completed using various approaches [24, 25, 26, 27, 28], but almost all NN training is accomplished via some variation on SGD: we compute (stochastic) gradient directions $\nabla \ell_{i_t}(w_t) := \nabla \ell(w_t, \{x_{i_t}, y_{i_t}\})$ that, on expectation, decrease the loss, and then set $w_{t+1} \leftarrow w_t - \eta \nabla \ell_{i_t}(w_t)$. Here, $\eta > 0$ is the learning rate, and i_t represents a mini-batch of examples, selected from X .

Why classical distributed approaches can be ineffective? Computing $\nabla \ell(w_t, X)$ over the whole X is wasteful [29]. Instead, mini batch SGD computes $w_{t+1} \leftarrow w_t - \eta \nabla \ell(w_t, X_{i_t})$ for a small subsample X_{i_t} of X . In a centralized system, we often use no more than a few hundred data items in X_{i_t} , and few would advocate using more than a few tens of thousands of X_{i_t} [13, 14, 16].

For distributed computation, this is problematic for two reasons: first, it makes it difficult to speed up the computation by adding more computing hardware. Since the batch size $|X_{i_t}|$ is small, splitting the task to more than a few compute nodes is no beneficial, which motivates different training approaches for NNs [30, 31, 32, 33, 34, 35]. Second, gathering the updates in a distributed setting introduces a non-negligible time overhead in large clusters, which is often the main bottleneck towards efficient large-scale computing — see Section 5. This imbalance between communication and computation capacity may lead to significant *increases* in training time when a larger cluster is used.

¹89% of cloud-based deep learning projects are executed on EC2, according to Amazon’s marketing materials.

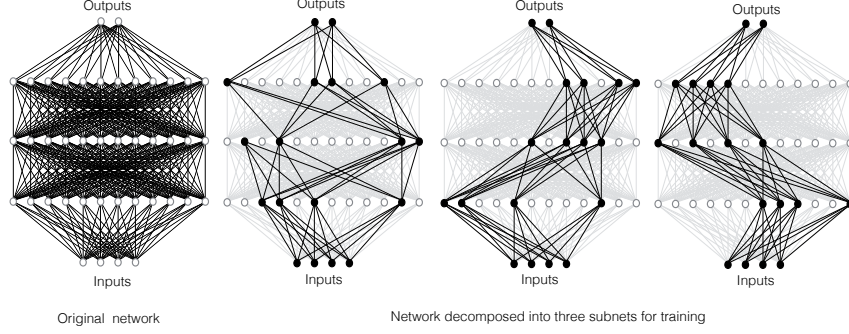


Figure 1: Decomposing a NN with three hidden layers into three subnets.

3 Training via Independent Subnetworks

Assume n sites in a distributed system. For simplicity, we assume all layers of the NN utilize the same activation function. Let f^l denote the vector of activations at layer l . f^t denotes the set of activations at the final or “top” layer of the network, and f^0 denotes the feature vector that is input into the network. Assume that the number of neurons at layer l is N_l . IST is a randomized, distributed training regime that utilizes a set of *membership indicators*:

$$\{m_{s,i}^l\}_{s \in \{1, \dots, n\}, i \in \{1, \dots, N_l\}}$$

Here, s ranges over the n sites, and i ranges over the neurons in layer l . Each $m_{s,i}^l \in \{0, 1\}$, is randomly selected, where the marginal probability is $\mathbb{P}[m_{s,i}^l = 1] = \frac{1}{n}$. Further, for each layer l and activation i , we constrain $\sum_s m_{s,i}^l$ to be 1 and the covariance of $m_{s,i}^l$ and $m_{s,i'}^{l-1}$ must be zero, so that $\mathbb{E}[m_{s,i}^l m_{s,i'}^{l-1}] = \frac{1}{n^2}$.

Then, we define the recurrence at the heart of IST:

$$\hat{f}^l = f\left(n^2 \sum_s m_s^l \odot \left(W^l \left(m_s^{l-1} \odot \hat{f}^{l-1}\right)\right)\right). \quad (2)$$

Here, W^l is the weight matrix connecting layer $l-1$ to layer l , and \odot denotes the Hadamard product of the two vectors. This recurrence is useful for two key reasons. First, it is easy to argue that if \hat{f}^{l-1} is an unbiased estimator for f^{l-1} , then $n^2 \sum_s m_s^l \odot \left(W^l \left(m_s^{l-1} \odot \hat{f}^{l-1}\right)\right)$, is an unbiased estimator for $W^l f^{l-1}$. To show this, we note that the j th entry in the vector $n^2 \sum_s m_s^l \odot \left(W^l \left(m_s^{l-1} \odot \hat{f}^{l-1}\right)\right)$ is computed as $n^2 \sum_s \sum_{i'} W_{j,i}^l m_{s,i'}^l m_{s,i}^{l-1} \hat{f}_i^{l-1}$, and hence its expectation is:

$$\begin{aligned} \mathbb{E}\left[n^2 \sum_s \sum_i \sum_{i'} W_{j,i}^l m_{s,i'}^l m_{s,i}^{l-1} \hat{f}_i^{l-1}\right] &= n^2 \sum_s \sum_i \sum_{i'} W_{j,i}^l \mathbb{E}\left[m_{s,i'}^l m_{s,i}^{l-1} \hat{f}_i^{l-1}\right] \\ &= n^2 \sum_s \sum_i \frac{1}{n^2} W_{j,i}^l \mathbb{E}\left[\hat{f}_i^{l-1}\right] = \sum_i W_{j,i}^l f_i^{l-1} \end{aligned}$$

which is precisely the j th entry in $W^l f^{l-1}$.

This unbiasedness suggests that this recurrence can be computed in place of the standard recurrence implemented by a NN, $f^l = f(W^l f^{l-1})$. A feature vector can be pushed through the resulting “approximate” NN, and the final vector \hat{f}^t can be used as an approximation for f^t .

3.1 Distributing Independent Subnets

The second reason the recurrence is useful is that it is much easier to distribute the computation of \hat{f}^t —and its backpropagation—than that of f^t . When randomly generating $\{m_{s,i}^l\}_{s \in \{1, \dots, n\}, i \in \{1, \dots, N_l\}}$, we require that $\sum_s m_{s,i}^l$ be 1. Two important aspects follow directly from this requirement. First, in the summation of Formula (2), only one “site” can contribute to the j th entry in the vector \hat{f}^l ; this is due

Algorithm 1 Independent subnet training.

```

1: Initialize weight matrices  $W^1, W^2, \dots, W^t$ 
2: while loss keeps improving do
3:   Sample  $\{m_{s,i}^t\}_{t \in \{1 \dots t-1\}, s \in \{1 \dots n\}, i \in \{1 \dots, N_l\}}$ 
4:   /* Execute local SGDs */
5:   for each site  $s$  do
6:     /* Send weights to local SGD */
7:     for each layer  $l$  do
8:       Compute  $\mathcal{W}_s^l = \{W_{i,j}^l\}_{s.t. m_{s,i}^l = 1, m_{s,j}^{l-1} = 1}$ 
9:       Send  $\mathcal{W}_s^l$  to site  $s$ 
10:    end for
11:    Run subnet local SGD at site  $s$ 
12:  end for
13:  /* Retreive results of local SGD */
14:  for each site  $s$ , layer  $l$  do
15:    Retrieve updated  $\mathcal{W}_s^l$  from site  $s$ 
16:    for each  $(i, j)$  s.t.  $m_{s,i}^l = 1, m_{s,j}^{l-1} = 1$  do
17:      Update  $W^l$  by replacing  $W_{i,j}^l$  with corresponding value from  $\mathcal{W}_s^l$ 
18:    end for
19:  end for
20: end while

```

to the Hadamard product with m_s^l , which implies that all other sites' contributions will be zeroed out. Second, only the entries in \hat{f}^{l-1} that were *themselves* associated with the same site value for s can contribute to the j th entry, again due to the Hadamard product with m_s^{l-1} .

This implies that we can co-locate at site s the computation of all entries in \hat{f}^{l-1} where $m_{s,i}^{l-1}$ is 1, and all entries in \hat{f}^l where $m_{s,i}^l$ is 1. *No cross-site communication is required to compute the activations in layer l from the activations in layer $l-1$.* Further, since only the entries in W_j for which $m_{s,i}^l/m_{s,i}^{l-1} = 1$ are used at site i —and on expectation, only $\frac{1}{n^2}$ of the weights in W^l will be used—this implies that during an iteration of distributed backpropagation, each site needs only (and communicates gradients for) a fraction $\frac{1}{n^2}$ of the weights in each weight matrix.

The distributed implementation of the recurrence across three sites for a NN with three hidden layers is depicted in Figure 1. The neurons in each layer are partitioned randomly across the sites, except for the input layer, which is fully utilized at all sites and the output layer, which computes all of the activations at the top layer.

3.2 Distributed Training Algorithm

This suggests an algorithm for distributed learning, given in Algorithm 1 and Algorithm 2. Algorithm 1 repeatedly samples a set of membership indicators, and then partitions the model weights across the set of compute nodes. Since the weights are fully partitioned, the independent subsets can be trained separately on local data for a number of iterations (Algorithm 2), before the indicators are re-sampled, and the weights are re-shuffled across the nodes. Note that periodic resampling of the indicators (followed by reshuffling) is necessary due to the possible accumulation of random effects. While the recurrence of Formula (2) provides for an unbiased estimate for the input to a neuron, after backpropagation, the expected input to a neuron will change. Since each subset is being trained using samples from the same data distribution, this shift may be inconsistent across sites. Resampling guards against this.

3.3 Correcting Distributional Shift

There is, however, a significant problem with the above formulation. Specifically, when justifying the use of the recurrence of Formula (2), we argued that since $n^2 \sum_s m_s^l \odot (W^l (m_s^{l-1} \odot \hat{f}^{l-1}))$ is an unbiased estimator for $W^l f^{l-1}$, it holds that $\hat{f}^l = f(n^2 \sum_s m_s^l \odot (W^l (m_s^{l-1} \odot \hat{f}^{l-1})))$ is

a reasonable estimator for $f^l = f(W^l f^{l-1})$. In doing so, we are guilty of applying a form of the classical statistical fallacy that for random variable x , if $\mathbb{E}[x] = b$, then $\mathbb{E}[f(x)] \approx f(b)$.

This fallacy is dangerous when the activation f is non-linear. Because the membership indicators force subsampling the inputs to each neuron (and a scale factor of n^2 is then applied to the resulting quantity to unbias it), we end up increasing the standard deviation of the input to each neuron by a factor of n during training, compared to the standard deviation that will be observed during inference, without the use of membership indicators. This increased variance means that we are more likely to observe extreme inputs to each neuron during training than during actual deployment. The network learns to expect such extreme values and avoid saturation during deployment, and adapts accordingly. However, the learned network fails when it is deployed.

To match the training and deployment distributions, we could apply an analytic approach. Instead, we simply remove the n^2 correction. I.e., during training, for a given neuron, we compute the mean μ and standard deviation σ of the inputs to the neuron, and use a modified activation function $f'(x) = f((x - \mu)/\sigma)$. Before inference, we can compute μ and σ for each neuron over a small subset of the training data using the full network, and use those values during deployment.

Note that this is equivalent to batch normalization [36]—we can learn a scale and shift as well. Though our motivation for its use is somewhat different. Classically, batch normalization keeps the input in the non-saturated range of the activation function during training. This tends to speed convergence and improve generalization. Yet, IST *will simply not work* without some sort of normalization, due to the distributional shift that will be encountered when deploying the whole network.

3.4 Why Is This Fast?

By subsampling, we reduce both network traffic and compute workload. In addition, IST allows for periods of local updates with no communication, again reducing network traffic.

For a feed-forward NN, at each round of “classical” data parallel training, the entire set of parameters must be broadcast to each site. Measuring the inflow to each site, the total network traffic per gradient step is (in floating point numbers transferred): $\sum_{i=1}^t nN_{i-1}N_i$. In contrast, during IST, each site receives the current parameters only one time every J gradient steps. Subsampling reduces this cost further; the matrices attached to the input and output layers are partitioned across nodes (not broadcast), and only a $\frac{1}{n}$ fraction of the weights in each of the other matrices are sent to any node. The total network traffic per gradient step is: $\frac{N_0N_1+N_{t-1}N_t}{J} + \sum_{i=1}^t \frac{N_{i-1}N_i}{n \times J}$.

Computational resource utilization is reduced similarly. Considering the FLOPs required by matrix multiplications during forward and backward steps, during “classical” data parallel training, the number of FLOPS required per gradient step is: $4 \sum_{i=1}^l BN_{i-1}N_i$. In contrast, the number of FLOPS per IST gradient step is: $4BN_0N_1 + 4BN_{t-1}N_t + 4B \sum_{i=1}^l \frac{N_{i-1}N_i}{n}$. Note that this also explains the reduction of RAM usage for IST, which enables training of larger models.

In Figure 2 we plot the average cost of each gradient step as a function of the number of machines, assuming a feed forward NN with three hidden layers of 4,000 neurons, an input feature vector of 1,000 features, a batch size of 512 data objects, and 200 output labels, assuming J , the number of subnet local SGD steps, is 10. There is a radical decrease in both network traffic and FLOPS using IST. In particular, using IST both of these quantities *decrease* with the addition of more machines in the cluster.

Note that this plot does not tell the whole story, as IST may have lower (or higher) statistical efficiency. The fact that IST partitions the network and runs local updates may decrease efficiency, whereas the fact that each “batch” processed during IST actually consists of n independent samples of size B (compared to a single global sample in classical data parallel training) may tends to increase efficiency. This will be examined experimentally.

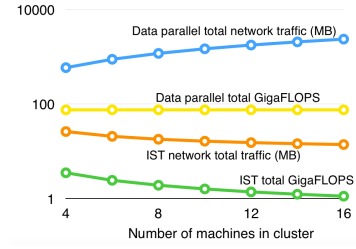


Figure 2: Comparing the cost of IST with data parallel learning.

3.5 IST for Non-Fully Connected Architectures

As described, IST applies to fully-connected layers. However, the idea as described here **can** still be applied to the fully-connected layer(s) that make part of nearly every modern architecture. For a straightforward extension, during training, the rest of the network is broadcast to every site, whereas the fully connected layers are decomposed into subnets. IST still has significant benefits as the fully-connected layer(s) tend to be the most expensive to move between sites during training. Consider the full ImageNet [37] for a deep model as ResNet50: the convolutional layers have 17,614,016 parameters (67.2MB, 28.2%), whereas the fully-connected layer at the top has 44,730,368 parameters (170.6MB, 71.8%) amenable to IST. We show that this simple extension results in significant speedup of training CNN over CIFAR100 and full ImageNet datasets. We discuss more advanced combination between IST and other recent work to further resolve this issue in section 5.

4 Empirical Evaluation

Learning tasks and environment. (1) *Google Speech Commands* [38]: We learn a 2-layer network of 4096 neurons and a 3-layer network of 8192 neurons to recognize 35 labeled keywords from audio waveforms (in contrast to the 12 keywords in prior reports [38]). We represent each waveform as a 4096-dimensional feature vector [39]. (2) *VGG on CIFAR100 and full ImageNet* [40]: We train the VGG image classification model (see Section 3.5 for a discussion of IST and non-fully connected architectures) over the benchmark datasets of CIFAR100 and full ImageNet; **we include the complete ImageNet dataset with all 21,841 categories and report the top-10 accuracy.** (3) *Amazon-670k* [41]: We train a 2-layer, fully-connected neural network, which accepts a 135,909-dimensional input feature, and generates a prediction over 670,091 output labels. Further details of the learning tasks and hyperparameter tuning description are enumerated in the appendix.

We train the Google speech networks on three AWS CPU clusters, with 2, 4, and 8 CPU instances (`m5.2xlarge`). We train the VGG model on CIFAR100 and full ImageNet and Amazon-670k extreme classification network on three AWS GPU clusters, with 2, 4, and 8 GPU machines (`p3.2xlarge`). Our choice of AWS was deliberate, as it is a very common learning platform, and *illustrates the challenge faced by many consumers*: distributed ML without a super-fast interconnect.

Distributed Implementation Notes. We implement a distributed parameter server for IST in PyTorch, the detailed description is attached in the appendix. We compare IST to the PyTorch implementation of data parallel learning. We also adapt the PyTorch data parallel learning to realize local SGD [23], where learning occurs locally for a number of iterations before synchronizing.

For the CPU experiments, we use PyTorch’s `gloo` backend. For the GPU experiments, data parallel learning and local SGD use PyTorch’s `nccl` backend, which leverages the most advanced Nvidia collective communication library (the set of high-performance multi-GPU and multi-node collective communication primitives optimized for NVIDIA GPUs). `nccl` implements ring-based all-reduce [22], which is used in well-known distributed learning systems such as Horovod [42].

Unfortunately, IST cannot use the `nccl` backend: it does not support the `scatter` operator required to implement IST, likely because the deep learning community has focused on data parallel learning. As a result, IST must use the `gloo` backend (meant for CPU-based learning). *This is a serious handicap for IST*, though we emphasize that it is not the result of any intrinsic flaw of the method, it is merely a lack of support for required operations in the high-performance GPU library. To give the reader an idea of the magnitude of this handicap, data parallel CIFAR100 VGG learning realizes a $3.1 \times$ speedup when switching from the `gloo` backend to `nccl` backend.

The experimental results are summarized below:

Scalability. We first investigate the relative scaling of IST compared to the alternatives, with an increasing number of EC2 workers. For various configurations we time how long each of the distributed learning frameworks take to complete one training epoch. Figure 3 gives the results.

Convergence speed. While IST can process data quickly, there are questions regarding its statistical efficiency vis-a-vis the other methods, and how this affects convergence. Figure 4 plots the hold-out test accuracy for selected benchmarks as a function of time. Table 1 shows the training time required for the various methods to reach specified levels of hold-out test accuracy.

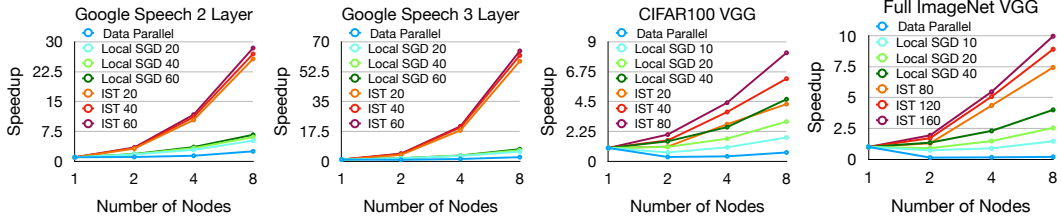


Figure 3: Scaling comparison of data parallel, local SGD and IST with various local update iterations. The speedup is calculated by comparing with the training time for one epoch to 1-worker SGD. The number after local SGD or IST legend represents the local update iterations.

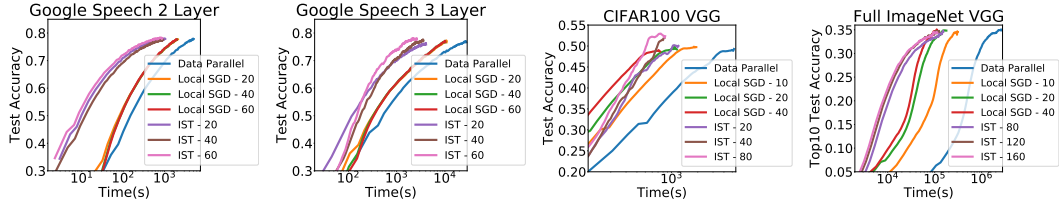


Figure 4: Test accuracy vs. time. 2/3-layer Google speech models are trained using an 8-CPU cluster; VGG on CIFAR100 is trained using 4-GPU cluster; VGG on full ImageNet is trained using a 8-GPU cluster. The number after local SGD or IST legend represents the local update iterations.

Trained model accuracy. Because IST is inherently a model-parallel training method, it has certain advantages, including the ability to scale to large models. We study the relationship between the embedding dimensions and the hold-out test performance for the Amazon-670k recommendation task in a 8-GPU cluster. The precision @1, @3, and @5 are reported in Table 2. In Table 3 we give the final accuracy of each method, trained on a 2-node cluster.

Discussion. There are a few takeaways from the experimental results. First, as expected, there are significant advantages to IST in terms of being able to process data quickly. Figure 3 shows that IST is able to process far more data in a short amount of time than the other distributed training algorithm. Interestingly, we find that the IST speedups in CPU clusters are more significant than that in GPU clusters. There are two reasons for this. First, for GPU clusters, IST suffers from its use of PyTorch’s gloo backend, compared to the all-reduce operator provided by nccl. Second, since the GPU

| Google Speech 2 Layer | | | | | | | | | |
|-----------------------|---------------|--------|--------|-----------|--------|--------|-------------|------------|-----------|
| | Data Parallel | | | Local SGD | | | IST | | |
| | 2 Node | 4 Node | 8 Node | 2 Node | 4 Node | 8 Node | 2 Node | 4 Node | 8 Node |
| Accuracy | 2 Node | 4 Node | 8 Node | 2 Node | 4 Node | 8 Node | 2 Node | 4 Node | 8 Node |
| 0.63 | 118 | 269 | 450 | 68 | 130 | 235 | 35 | 28 | 24 |
| 0.75 | 759 | 1708 | 2417 | 444 | 742 | 1110 | 231 | 167 | 192 |
| Google Speech 3 Layer | | | | | | | | | |
| | Data Parallel | | | Local SGD | | | IST | | |
| | 2 Node | 4 Node | 8 Node | 2 Node | 4 Node | 8 Node | 2 Node | 4 Node | 8 Node |
| Accuracy | 2 Node | 4 Node | 8 Node | 2 Node | 4 Node | 8 Node | 2 Node | 4 Node | 8 Node |
| 0.63 | 376 | 1228 | 1922 | 182 | 586 | 1115 | 76 | 141 | 300 |
| 0.75 | 4534 | 9340 | 14886 | 2032 | 4107 | 6539 | 812 | 664 | 1161 |
| CIFAR100 | | | | | | | | | |
| | Data Parallel | | | Local SGD | | | IST | | |
| | 2 Node | 4 Node | 8 Node | 2 Node | 4 Node | 8 Node | 2 Node | 4 Node | 8 Node |
| Accuracy | 2 Node | 4 Node | 8 Node | 2 Node | 4 Node | 8 Node | 2 Node | 4 Node | 8 Node |
| 0.36 | 108 | 275 | 730 | 23 | 67 | 133 | 17 | 39 | 212 |
| 0.48 | 542 | 1472 | 3342 | 104 | 215 | 473 | 68 | 85 | 466 |
| Full ImageNet | | | | | | | | | |
| | Data Parallel | | | Local SGD | | | IST | | |
| | 2 Node | 4 Node | 8 Node | 2 Node | 4 Node | 8 Node | 2 Node | 4 Node | 8 Node |
| Accuracy | 2 Node | 4 Node | 8 Node | 2 Node | 4 Node | 8 Node | 2 Node | 4 Node | 8 Node |
| 0.20 | 108040 | 278542 | 504805 | 6900 | 14698 | 30441 | 3629 | 4379 | 5954 |
| 0.26 | 225911 | 393279 | 637188 | 15053 | 22055 | 39439 | 6189 | 7711 | 10622 |

Table 1: The time (in seconds) to reach various levels of accuracy.

provides a very high level of computation, there is less benefit to be realized from the reduction in FLOPS per gradient step using IST (as the GPU does not appear to be compute bound).

Figure 4 and Table 1 generally show that IST is much faster compared to the other frameworks for achieving high levels of accuracy on a hold-out test set. For example, IST exhibits a $4.2 \times$ speedup compared to local SGD, and $10.6 \times$ speedup compared to classical data parallel for the 2-layer Google speech model to reach 77%. IST exhibits $6.1 \times$ speedup compared to local SGD, and a $16.6 \times$ speedup comparing to data parallel for the 3-layer model to reach the accuracy of 77%. Note that this was observed even though IST was handicapped by its use of `gloo` for its GPU implementation.

Another key advantage of IST is illustrated in Table 2; because it is a model-parallel framework and distributes the model to multiple machines, IST is able to scale to virtually unlimited model sizes. In this case, it can compute 2560-dimensional embedding in 8-GPU cluster (and realize the associated, additional accuracy) whereas the data parallel approaches are unable to do this.

| | Data Parallel | Local SGD | IST |
|------|---------------|-----------|---------------|
| 512 | 0.3861 | 0.3454 | 0.3164 |
| 1024 | | Fail | 0.4089 |
| 1536 | | Fail | 0.4320 |
| 2048 | | Fail | 0.4365 |
| 2560 | | Fail | 0.4384 |
| | | | 0.3944 |
| | | | 0.3658 |

Table 2: Precision @1, @3, @5 on the Amazon 670k benchmark.

It is interesting that *most of the frameworks actually do worse with additional machines*. This illustrates a significant problem with distributed learning. Unless a super-fast interconnect is used (and such interconnects are not available from typical cloud

providers), it can actually be *detrimental* to add additional machines, as the added cost of transferring data can actually result in *slower* running times. We see this clearly in Table 1, where the state-of-the-art PyTorch data parallel implementation (and the local SGD variant) does significantly *worse* with more machines. IST is the only of the three frameworks to show the ability to utilize additional machines without actually becoming much slower or slower to reach high accuracy. That said, even IST struggled to scale beyond two machines in the case of VGG image classification (since IST does not decompose the convolutional layers into subnets). Still, IST showed the best potential to scale.

Finally, various compression schemes can be used to increase the bandwidth of the interconnect (e.g., gradient sparsification [43], quantization [44], sketching [45], and low-rank compression [46]). However, these methods could be used with *any* framework—including IST. We conjecture that while compression may allow effective scaling to larger clusters, it would not affect the efficacy of IST.

5 Related work

Data parallelism suffers from the high bandwidth costs to communicate gradients between workers. Quantized SGD [44, 47, 48] and sparsified SGD [43] both address this. Quantized SGD uses lossy compression to quantize the gradients [49, 50, 51, 44, 52]. Sparsified SGD transmits only the gradients with maximal magnitude. Such methods are orthogonal to IST.

Distributed local SGD [53, 54, 55, 56] updates the parameters, through averaging, only after several local steps are performed. This reduces synchronization and allows higher hardware efficiency [56]. IST uses a similar approach but makes the local SGD and each synchronization round less expensive. Further, the non-overlapping partitions of IST enables more aggressive local update period.

Finally, there is recent work in aid to extend IST to non-fully connected architectures. [57] proposes to split the training of deep CNNs into a stack of gradient-isolated modules. IST can be ideally applied on the head FC layers.

6 Conclusion

In this work, we propose *independent subnet training* for distributed training of fully connected NNs. By stochastically partitioning the model into non-overlapping subnets, IST reduces the communication

overhead for model synchronization, and the computation workload of forward-backward propagation for a thinner model on each worker. This results in two advances: *i*) IST significantly accelerates the training process comparing with standard data parallel approaches for distributed learning, and *ii*) IST scales to large models that cannot be learned using standard data parallel approaches.

Broader Impact

Machine learning is no longer a niche area. Neural networks are now used by almost every discipline and sub-discipline of science and engineering, as well as by almost every industry and sub-industry. As dataset becomes larger and larger, all of those consumers of neural network technology will have a need to reduce training time and explore larger models, using parallel or distributed computing. Unfortunately, there are no reliable, out-of-the-box solutions to make this happen. Attempts to move from one machine to many often meet with slowdowns, rather than speedups in commercial cloud platforms such as Amazon EC2. According to Amazon’s marketing materials, 89% of cloud-based deep learning projects are executed on EC2. With so many consumers of this platform — who are not expert in machine learning or distributed computing — there is a pressing need to develop distributed training methods that “just work.” In this paper, we propose a distributed training algorithm that makes it easy for all of these consumers of neural network technology to achieve real speedups with minimal expertise in commercial cloud platforms.

References

- [1] Alexander Ratner, Dan Alistarh, Gustavo Alonso, Peter Bailis, Sarah Bird, Nicholas Carlini, Bryan Catanzaro, Eric Chung, Bill Dally, Jeff Dean, et al. SysML: The new frontier of machine learning systems. *arXiv preprint arXiv:1904.03257*, 2019.
- [2] Jeffrey Dean, Greg Corrado, Rajat Monga, Kai Chen, Matthieu Devin, Mark Mao, Andrew Senior, Paul Tucker, Ke Yang, Quoc V Le, et al. Large scale distributed deep networks. In *Advances in neural information processing systems*, pages 1223–1231, 2012.
- [3] Trishul M Chilimbi, Yutaka Suzue, Johnson Apacible, and Karthik Kalyanaraman. Project Adam: Building an efficient and scalable deep learning training system. In *OSDI*, volume 14, pages 571–582, 2014.
- [4] Mu Li, David G Andersen, Jun Woo Park, Alexander J Smola, Amr Ahmed, Vanja Josifovski, James Long, Eugene J Shekita, and Bor-Yiing Su. Scaling distributed machine learning with the parameter server. In *OSDI*, volume 14, pages 583–598, 2014.
- [5] Stefan Hadjis, Ce Zhang, Ioannis Mitliagkas, Dan Iter, and Christopher Ré. Omnivore: An optimizer for multi-device deep learning on CPUs and GPUs. *arXiv preprint arXiv:1606.04487*, 2016.
- [6] Xiru Zhang, Michael Mckenna, Jill P Mesirov, and David L Waltz. An efficient implementation of the back-propagation algorithm on the connection machine CM-2. In *Advances in neural information processing systems*, pages 801–809, 1990.
- [7] Philipp Farber and Krste Asanovic. Parallel neural network training on multi-spert. In *Algorithms and Architectures for Parallel Processing, 1997. ICAPP 97., 1997 3rd International Conference on*, pages 659–666. IEEE, 1997.
- [8] Rajat Raina, Anand Madhavan, and Andrew Y Ng. Large-scale deep unsupervised learning using graphics processors. In *Proceedings of the 26th annual international conference on machine learning*, pages 873–880. ACM, 2009.
- [9] Martín Abadi, Paul Barham, Jianmin Chen, Zhifeng Chen, Andy Davis, Jeffrey Dean, Matthieu Devin, Sanjay Ghemawat, Geoffrey Irving, Michael Isard, et al. Tensorflow: A system for large-scale machine learning. In *12th {USENIX} Symposium on Operating Systems Design and Implementation ({OSDI} 16)*, pages 265–283, 2016.
- [10] Adam Paszke, Sam Gross, Soumith Chintala, Gregory Chanan, Edward Yang, Zachary DeVito, Zeming Lin, Alban Desmaison, Luca Antiga, and Adam Lerer. Automatic differentiation in pytorch. 2017.

- [11] Linjian Ma, Gabe Montague, Jiayu Ye, Zhewei Yao, Amir Gholami, Kurt Keutzer, and Michael W Mahoney. Inefficiency of K-FAC for large batch size training. *arXiv preprint arXiv:1903.06237*, 2019.
- [12] Noah Golmant, Nikita Vemuri, Zhewei Yao, Vladimir Feinberg, Amir Gholami, Kai Rothauge, Michael W Mahoney, and Joseph Gonzalez. On the computational inefficiency of large batch sizes for stochastic gradient descent. *arXiv preprint arXiv:1811.12941*, 2018.
- [13] Priya Goyal, Piotr Dollár, Ross Girshick, Pieter Noordhuis, Lukasz Wesolowski, Aapo Kyrola, Andrew Tulloch, Yangqing Jia, and Kaiming He. Accurate, large minibatch SGD: training ImageNet in 1 hour. *arXiv preprint arXiv:1706.02677*, 2017.
- [14] Omry Yadan, Keith Adams, Yaniv Taigman, and Marc'Aurelio Ranzato. Multi-GPU training of convnets. *arXiv preprint arXiv:1312.5853*, 2013.
- [15] Yang You, Igor Gitman, and Boris Ginsburg. Scaling SGD batch size to 32K for ImageNet training. *arXiv preprint arXiv:1708.03888*, 2017.
- [16] Samuel L Smith, Pieter-Jan Kindermans, Chris Ying, and Quoc V Le. Don't decay the learning rate, increase the batch size. *arXiv preprint arXiv:1711.00489*, 2017.
- [17] Valeriu Codreanu, Damian Podareanu, and Vikram Saletore. Scale out for large minibatch SGD: Residual network training on ImageNet-1K with improved accuracy and reduced time to train. *arXiv preprint arXiv:1711.04291*, 2017.
- [18] Yang You, Jing Li, Jonathan Hseu, Xiaodan Song, James Demmel, and Cho-Jui Hsieh. Reducing BERT pre-training time from 3 days to 76 minutes. *arXiv preprint arXiv:1904.00962*, 2019.
- [19] Yang You, Jonathan Hseu, Chris Ying, James Demmel, Kurt Keutzer, and Cho-Jui Hsieh. Large-batch training for LSTM and beyond. *arXiv preprint arXiv:1901.08256*, 2019.
- [20] Nitish Srivastava, Geoffrey Hinton, Alex Krizhevsky, Ilya Sutskever, and Ruslan Salakhutdinov. Dropout: a simple way to prevent neural networks from overfitting. *The Journal of Machine Learning Research*, 15(1):1929–1958, 2014.
- [21] Petros Drineas, Ravi Kannan, and Michael W Mahoney. Fast monte carlo algorithms for matrices i: Approximating matrix multiplication. *SIAM Journal on Computing*, 36(1):132–157, 2006.
- [22] Nccl based multi-gpu training. <http://on-demand.gputechconf.com/gtc-cn/2018/pdf/CH8209.pdf>, 2018. Accessed: 2020-02-06.
- [23] Tao Lin, Sebastian U Stich, and Martin Jaggi. Don't use large mini-batches, use local SGD. *arXiv preprint arXiv:1808.07217*, 2018.
- [24] Stephen Wright and Jorge Nocedal. Numerical optimization. *Springer Science*, 35(67-68):7, 1999.
- [25] Matthew D Zeiler. Adadelta: an adaptive learning rate method. *arXiv preprint arXiv:1212.5701*, 2012.
- [26] Diederik P Kingma and Jimmy Ba. Adam: A method for stochastic optimization. *arXiv preprint arXiv:1412.6980*, 2014.
- [27] John Duchi, Elad Hazan, and Yoram Singer. Adaptive subgradient methods for online learning and stochastic optimization. *Journal of Machine Learning Research*, 12(Jul):2121–2159, 2011.
- [28] Sebastian Ruder. An overview of gradient descent optimization algorithms. *arXiv preprint arXiv:1609.04747*, 2016.
- [29] Aaron Defazio and Léon Bottou. On the ineffectiveness of variance reduced optimization for deep learning. *arXiv preprint arXiv:1812.04529*, 2018.
- [30] Albert S Berahas, Raghu Bollapragada, and Jorge Nocedal. An investigation of Newton-sketch and subsampled Newton methods. *arXiv preprint arXiv:1705.06211*, 2017.
- [31] Léon Bottou, Frank E Curtis, and Jorge Nocedal. Optimization methods for large-scale machine learning. *Siam Review*, 60(2):223–311, 2018.
- [32] Sudhir B Kylasa, Farbod Roosta-Khorasani, Michael W Mahoney, and Ananth Grama. GPU accelerated sub-sampled Newton's method. *arXiv preprint arXiv:1802.09113*, 2018.

[33] Peng Xu, Farbod Roosta-Khorasani, and Michael W Mahoney. Newton-type methods for non-convex optimization under inexact hessian information. *arXiv preprint arXiv:1708.07164*, 2017.

[34] Albert S Berahas, Majid Jahani, and Martin Takáč. Quasi-Newton methods for deep learning: Forget the past, just sample. *arXiv preprint arXiv:1901.09997*, 2019.

[35] James Martens and Roger Grosse. Optimizing neural networks with Kronecker-factored approximate curvature. In *International conference on machine learning*, pages 2408–2417, 2015.

[36] Sergey Ioffe and Christian Szegedy. Batch normalization: Accelerating deep network training by reducing internal covariate shift. In *International Conference on Machine Learning*, pages 448–456, 2015.

[37] A. Krizhevsky, I. Sutskever, and G. Hinton. Imagenet classification with deep convolutional neural networks. In *Advances in neural information processing systems*, pages 1097–1105, 2012.

[38] Pete Warden. Speech commands: A dataset for limited-vocabulary speech recognition. *arXiv preprint arXiv:1804.03209*, 2018.

[39] Stanley Smith Stevens, John Volkmann, and Edwin B Newman. A scale for the measurement of the psychological magnitude pitch. *The Journal of the Acoustical Society of America*, 8(3):185–190, 1937.

[40] K. Simonyan and A. Zisserman. Very deep convolutional networks for large-scale image recognition. *arXiv preprint arXiv:1409.1556*, 2014.

[41] Kush Bhatia, Kunal Dahiya, Himanshu Jain, Yashoteja Prabhu, and Manik Varma. *The Extreme Classification Repository: Multi-label Datasets and Code*. <http://manikvarma.org/downloads/XC/XMLRepository.html>.

[42] Alexander Sergeev and Mike Del Balso. Horovod: fast and easy distributed deep learning in tensorflow. *arXiv preprint arXiv:1802.05799*, 2018.

[43] Alham Fikri Aji and Kenneth Heafield. Sparse communication for distributed gradient descent. *arXiv preprint arXiv:1704.05021*, 2017.

[44] Dan Alistarh, Demjan Grubic, Jerry Li, Ryota Tomioka, and Milan Vojnovic. QSGD: Communication-efficient SGD via gradient quantization and encoding. In *Advances in Neural Information Processing Systems*, pages 1709–1720, 2017.

[45] Nikita Ivkin, Daniel Rothchild, Enayat Ullah, Ion Stoica, Raman Arora, et al. Communication-efficient distributed sgd with sketching. In *Advances in Neural Information Processing Systems*, pages 13144–13154, 2019.

[46] Thijs Vogels, Sai Praneeth Karimireddy, and Martin Jaggi. Powersgd: Practical low-rank gradient compression for distributed optimization. In *Advances in Neural Information Processing Systems*, pages 14236–14245, 2019.

[47] Matthieu Courbariaux, Yoshua Bengio, and Jean-Pierre David. BinaryConnect: Training deep neural networks with binary weights during propagations. In *Advances in neural information processing systems*, pages 3123–3131, 2015.

[48] Frank Seide, Hao Fu, Jasha Droppo, Gang Li, and Dong Yu. 1-bit stochastic gradient descent and its application to data-parallel distributed training of speech DNNs. In *Fifteenth Annual Conference of the International Speech Communication Association*, 2014.

[49] Tim Dettmers. 8-bit approximations for parallelism in deep learning. *arXiv preprint arXiv:1511.04561*, 2015.

[50] Suyog Gupta, Ankur Agrawal, Kailash Gopalakrishnan, and Pritish Narayanan. Deep learning with limited numerical precision. In *International Conference on Machine Learning*, pages 1737–1746, 2015.

[51] Itay Hubara, Matthieu Courbariaux, Daniel Soudry, Ran El-Yaniv, and Yoshua Bengio. Quantized neural networks: Training neural networks with low precision weights and activations. *Journal of Machine Learning Research*, 18(187):1–30, 2017.

[52] Wei Wen, Cong Xu, Feng Yan, Chunpeng Wu, Yandan Wang, Yiran Chen, and Hai Li. Terngrad: Ternary gradients to reduce communication in distributed deep learning. In *Advances in neural information processing systems*, pages 1509–1519, 2017.

[53] Ryan McDonald, Mehryar Mohri, Nathan Silberman, Dan Walker, and Gideon S Mann. Efficient large-scale distributed training of conditional maximum entropy models. In *Advances in Neural Information Processing Systems*, pages 1231–1239, 2009.

[54] Martin Zinkevich, Markus Weimer, Lihong Li, and Alex J Smola. Parallelized stochastic gradient descent. In *Advances in neural information processing systems*, pages 2595–2603, 2010.

[55] Ce Zhang and Christopher Ré. Dismwitted: A study of main-memory statistical analytics. *Proceedings of the VLDB Endowment*, 7(12):1283–1294, 2014.

[56] Jian Zhang, Christopher De Sa, Ioannis Mitliagkas, and Christopher Ré. Parallel SGD: When does averaging help? *arXiv preprint arXiv:1606.07365*, 2016.

[57] Sindy Löwe, Peter O’Connor, and Bastiaan Veeling. Putting an end to end-to-end: Gradient-isolated learning of representations. In *Advances in Neural Information Processing Systems*, pages 3033–3045, 2019.

[58] Alex Krizhevsky. One weird trick for parallelizing convolutional neural networks. *arXiv preprint arXiv:1404.5997*, 2014.

[59] Laurent Dinh, Razvan Pascanu, Samy Bengio, and Yoshua Bengio. Sharp minima can generalize for deep nets. In *Proceedings of the 34th International Conference on Machine Learning-Volume 70*, pages 1019–1028. JMLR. org, 2017.

[60] Nitish Shirish Keskar, Dheevatsa Mudigere, Jorge Nocedal, Mikhail Smelyanskiy, and Ping Tak Peter Tang. On large-batch training for deep learning: Generalization gap and sharp minima. *arXiv preprint arXiv:1609.04836*, 2016.

[61] Zhewei Yao, Amir Gholami, Qi Lei, Kurt Keutzer, and Michael W Mahoney. Hessian-based analysis of large batch training and robustness to adversaries. In *Advances in Neural Information Processing Systems*, pages 4949–4959, 2018.

[62] Jakub Konečný, H Brendan McMahan, Daniel Ramage, and Peter Richtárik. Federated optimization: Distributed machine learning for on-device intelligence. *arXiv preprint arXiv:1610.02527*, 2016.

[63] Brendan McMahan, Eider Moore, Daniel Ramage, Seth Hampson, and Blaise Aguera y Arcas. Communication-efficient learning of deep networks from decentralized data. In *Artificial Intelligence and Statistics*, pages 1273–1282, 2017.

Appendix

Implementation Details

We implement independent subnet training in PyTorch. In addition to IST, we use the default data parallel implementation provided by PyTorch; we also implement local SGD in PyTorch according to the algorithm proposed by [23].

Distributed Parameter Server. To support the IST algorithm, a carefully designed distributed system is required. Algorithm 1 implies that there is a coordinator, but in practice there can be no actual coordinator—a coordinator will inevitably become a bottleneck during learning. In our implementation of IST, we shard each weight matrix across all worker nodes. To run each invocation of subnet local SGD, each worker obtains a portion of each weight matrix from each of the other workers, runs subnet local SGD, and then returns the updated portions to their owners.

This requires an algorithm for distributed generation of membership indicators. Imagine a site s is assigned a set of neurons S_l at layer l and S_{l+1} at layer $l+1$; s will need all weights connecting any pairs of neurons in S_l and S_{l+1} . Site s and site s' may both have relevant weights, but for s' to send those weights to s , both will need to agree on S_l and S_{l+1} , ideally without incurring the cost of communicating indicators (which may be as high as sending the weights).

We use the simple idea of using a common pseudo-random number generator for all sites. A seed is broadcast, and that seed is used to produce identical pseudo-random sequences (and hence identical assignments) at all sites. Then, when site s' sends weights to site s , the latter need not specify which weights to send, nor receive any meta-data.

AWS EC2 Cluster Setting. To evaluate the performance of IST in commercial cloud platforms, we include the following clusters settings: i) CPU-clusters, associated with 2, 4, or 8 `m5.2xlarge` instances; ii) GPU-clusters, associated with 2, 4, or 8 `p3.2xlarge` instances. Each `m5.2xlarge` instance includes 8 virtual CPUs, and 32 GB memory. Each `p3.2xlarge` instance includes 1 Nvidia Tesla V100 GPU. The network bandwidth between instances is up to 10 Gbps for both CPU and GPU clusters.

We train the 2-/3- layer Google speech recognition networks on 2, 4, and 8 instance CPU clusters, the Amazon-670k product recommendation, VGG for CIFAR100 and full ImageNet on 2, 4, and 8 instance GPU clusters.

Benchmark Details

We enumerate more details of the benchmark applications we included in the empirical study as below.

(1) *Google Speech Commands* [38]: We learn a 2 -layer network of 4096 neurons and a 3-layer network of 8192 neurons to recognize 35 labeled keywords from audio waveforms (in contrast to the 12 keywords in prior report [38]). We represent each waveform as a 4096-dimensional feature vector [39]. There are 76,364 samples in the training set and 19,030 samples in the test set.

(2) *VGG on CIFAR100 and full ImageNet* [40]: We train the VGG image classification model over the benchmark datasets of CIFAR100 and Full Imagenet; **we include the complete imagenet dataset with all 21,841 categories and report the top-10 accuracy**. We want to emphasize that since we apply a combined approach for training convolutional neural networks (see Section 3.5 for a discussion of IST and non-fully connected architectures), the focus of the empirical study is to explore the **speedup introduced by IST for the top FC layers**. Choosing the best convolutional architecture (eg., ResNet, MobileNet, etc.) to extract image features is beyond the scope of this paper. Additionally, it is worth to mention that the classification on the full ImageNet dataset (with 14,197,122 images belong to 21,841 categories with heavily biased distribution) is far more challenging comparing to the more popular 1000 class ILSVRC benchmark. For the full ImageNet dataset, there are 12,777,410 samples in the training set and 1,419,712 samples in the test set.

(3) *Amazon-670k* [41]: We train a 2-layer, fully-connected neural network, which accepts a 135,909-dimensional input feature, and generates a prediction over 670,091 output labels. There are 490,449 samples in the training set and 153,025 samples in the test set.

We enumerate the model structure in Table 4.

| Speech 2 layer NN | | CIFAR100 VGG | | Full Imagenet VGG | |
|--------------------------|--------------------|--------------|--------------------|-------------------|---------------------|
| Layer | Parameters | Layer | Parameters | Layer | Parameters |
| fc1 | 4096×4096 | conv1 | $3 \times 3, 64$ | conv1 | $3 \times 3, 64$ |
| fc2 | 4096×4096 | conv2 | $3 \times 3, 128$ | conv2 | $3 \times 3, 128$ |
| Speech 3 layer NN | | conv3 | $3 \times 3, 256$ | conv3 | $3 \times 3, 256$ |
| Layer | Parameters | conv4 | $3 \times 3, 256$ | conv4 | $3 \times 3, 256$ |
| fc1 | 4096×8192 | conv5 | $3 \times 3, 512$ | conv5 | $3 \times 3, 512$ |
| fc2 | 8192×8192 | conv6 | $3 \times 3, 512$ | conv6 | $3 \times 3, 512$ |
| fc3 | 8192×4096 | conv7 | $3 \times 3, 512$ | conv7 | $3 \times 3, 512$ |
| Amazon-670k XML | | conv8 | $3 \times 3, 512$ | conv8 | $3 \times 3, 512$ |
| Layer | Parameters | fc1 | 512×4096 | fc1 | 512×8192 |
| fc1 | $135909 \times D$ | fc2 | 4096×4096 | fc2 | 8192×21841 |
| fc2 | $D \times 670091$ | fc3 | 4096×100 | | |

Table 4: Model Architecture of all the benchmark applications.

Hyper Parameter Tuning. We use the standard SGD method for all the models.

For 2-/3- layer google speech model, we choose the learning rate $\eta = 10^{-2}$ from an exponentially-spaced set $\{10^{-4}, 10^{-3}, 10^{-2}, 10^{-1}, 1\}$.

For Amazon-670k product recommendation tasks, we choose the learning rate $\eta = 1.0$ from an exponentially-spaced set $\{10^{-3}, 10^{-2}, 10^{-1}, 1, 10\}$.

For VGG on CIFAR100, we choose the initial learning rate 10^{-2} from an exponentially-spaced set $\{10^{-3}, 10^{-2}, 10^{-1}, 1\}$ and decayed once by the factor of 0.1 after 30 epochs.

For VGG on full ImageNet, we choose the initial learning rate 10^{-2} from an exponentially-spaced set $\{10^{-3}, 10^{-2}, 10^{-1}\}$ and decayed once by the factor of 0.3 after 15 epochs. Due to the various image sizes appearing in the full ImageNet dataset, we downsample all the images to a fixed size of 32×32 .

The initialization of the neural networks were completed by the default initialization in PyTorch. We only consider single run experiments, due to the fact that there are plenty of distributed configurations (eg., cluster size, local sgd iterations) we explore and report in this paper. To give the reader an idea of the time of running these experiments, we roughly spent 300 hours CPU instance credit and more than 10,000 hours GPU instance credit for all the benchmarks.

Complete Experimental Results

Due to the space limits, the complete experiments are included in this appendix. The hold-out test accuracy for different distributed settings are enumerated in Figure 5 for 2- layer google speech model, Figure 6 for 3-layer google speech model, Figure 7 for VGG on CIFAR100, and Figure 8 for VGG on full ImageNet.

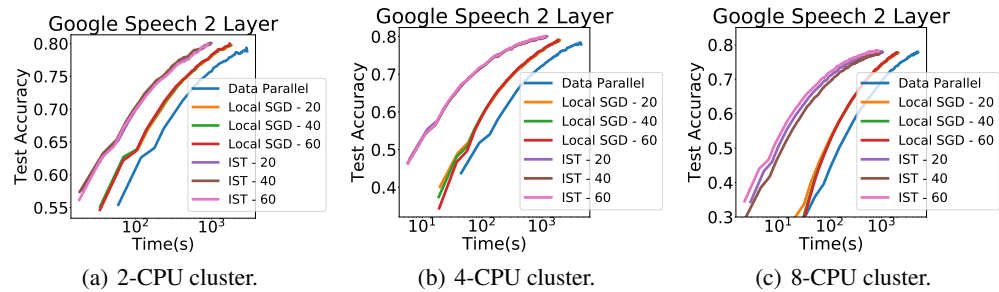
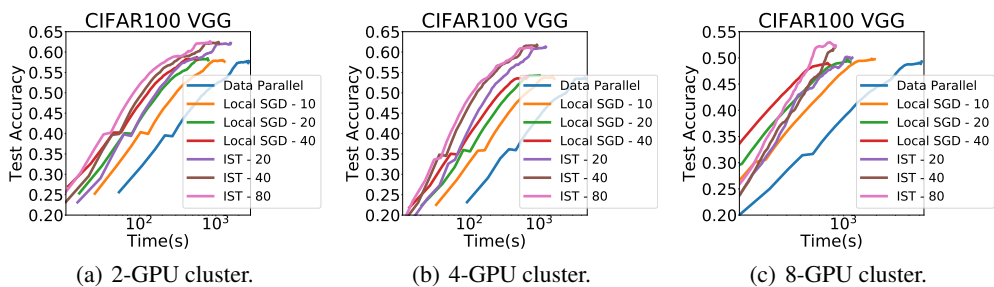
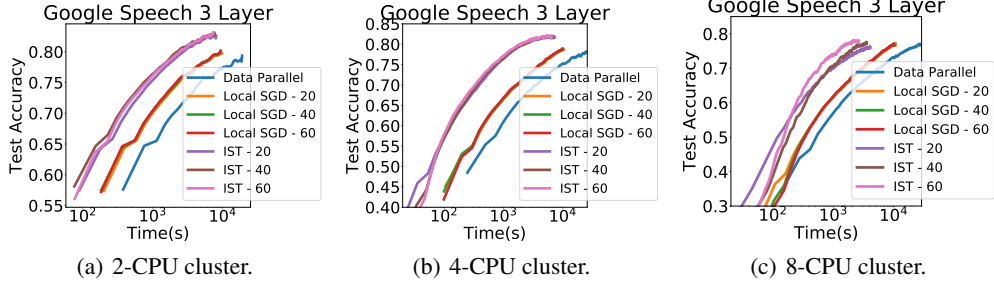


Figure 5: Hold-out test accuracy observed as a function of time (in log-scale). 2-layer google speech models are trained over 2, 4, 8 node CPU clusters.



Extended Related work

Data parallelism and model parallelism are two approaches to distribute the training computation. In model parallelism, each worker in the cluster is responsible for the computations in different parts of a neural network, for example, different layer in the model can be assigned to a different worker [58]. While in data parallelism, every worker has a complete copy of the model and conducts the computation on different data batches.

Data parallelism often suffers from the high bandwidth costs to communicate gradient updates between workers. Quantized SGD [44, 47, 48] and sparsified SGD [43] both address this. Quantized SGD uses lossy compression to quantize the gradients [49, 50, 51, 44]; in some extreme cases, to only three numerical levels [52]. Sparsified SGD reduces the exchange overhead by transmitting the gradients with maximal magnitude. Although such methods are relevant to our approach, there is a fundamental difference: those techniques post-process the full-model gradients from the forward and backward propagation of the raw model, which is computational demanding; while our approach only compute the gradients of a thin partitioned model, so that computation cost is also reduced. Additionally, these compression approaches can also be leveraged by IST in transmit model updates.

Recently, there has been a series of papers on using parallelism to “*Solve the YY learning problem in XX minutes*”, for ever-decreasing values of XX [13, 14, 15, 16, 17, 18, 19]. Often these methods employ large batches. It is generally accepted—though still debated [59]—that large batch training converges to “sharp minima”, hurting generalization [60, 61, 29]. Further, achieving such results seems to require teams of PhDs utilizing special-purpose hardware: there is no “plug-n-play” approach that generalizes well without extensive experimental trial-and-error.

Distributed local SGD [53, 54, 55, 56] updates the parameters, through averaging, only after several local steps are performed per compute node. This reduces synchronization and thus allows for higher hardware efficiency [56]. IST uses a similar approach but makes the local SGD and each synchronization round less expensive. Recent approaches [23] propose less frequent synchronization towards the end of the training, but they cannot avoid it at the beginning. As the experiments in [23] reveal, local updates of the whole model leads to interdependence among updates, which limits the local updates up to 16 iterations, while IST enables much more aggressive local update period.

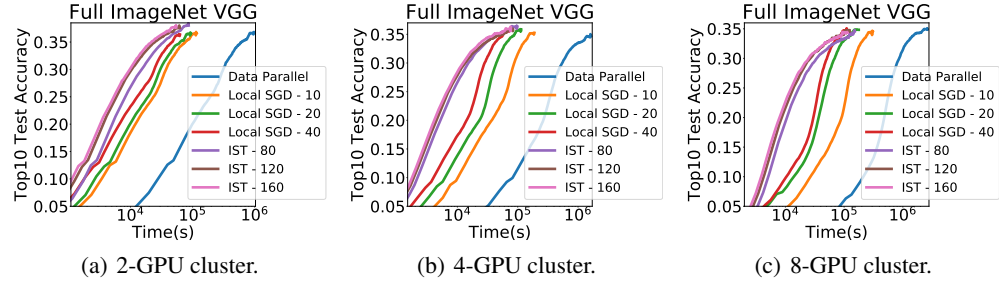


Figure 8: Hold-out top10 test accuracy observed as a function of time (in log-scale). VGG model on full ImageNet are trained over 2, 4, 8 node GPU clusters.

Additionally, the non-overlapping partition of the model by IST enables more aggressive local update period.

Federated learning, first proposed by Google [62, 63], has drawn increasing attention, which is defined as a problem of training a high-quality shared global model with a central server from decentralized data scattered among a large number of clients. Although IST is not initially proposed for federated learning, it will be interesting to extend IST for communication/computation-light, energy-frugal environment, as in mobile edge-computing.